A cobalt(III) complex as a dual-modal probe for the detection of sodium dithionite via MRI and fluorescence

Jiaqi Zhou,[a] Zexiao Huang,[a] Haoyan Xing,[a] Yue Wang,[a,*] Cheng Zhang,[a] Zhuye Shang,[a] Qingtao Meng,[a,b,*] Run Zhang,[c] Zhiqiang Zhang,[b,*]

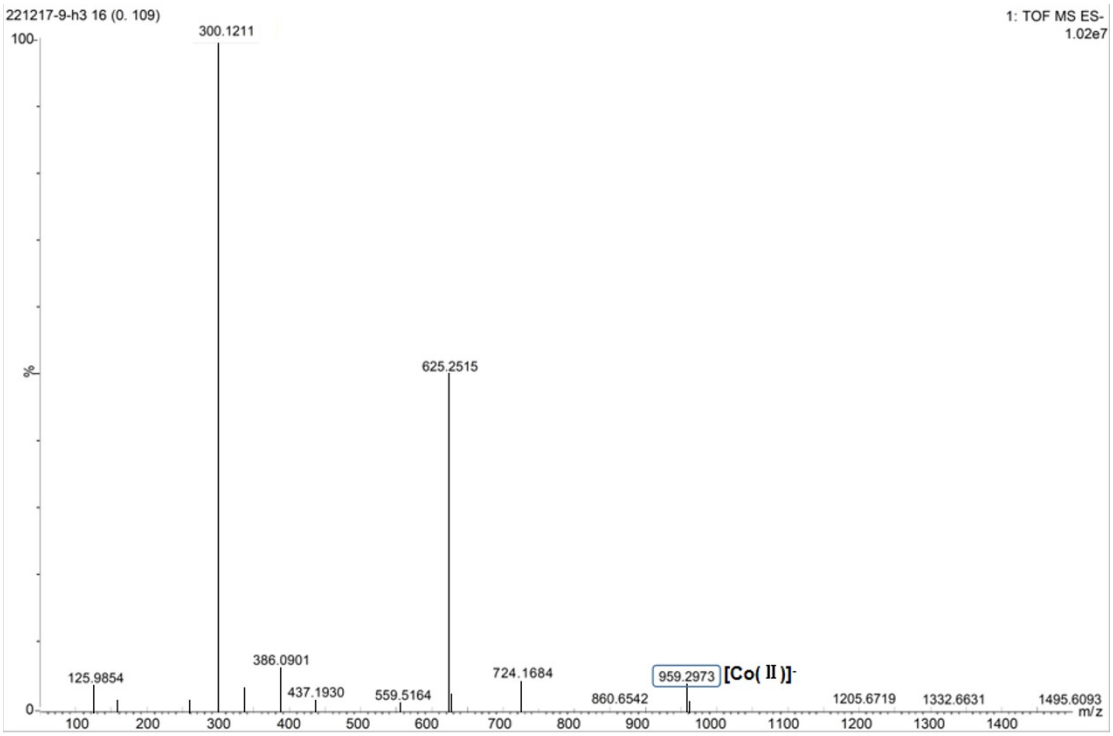

Fig. S1 Mechanism diagram of the mass spectrum after identifying sodium dithionite with probe **H1**

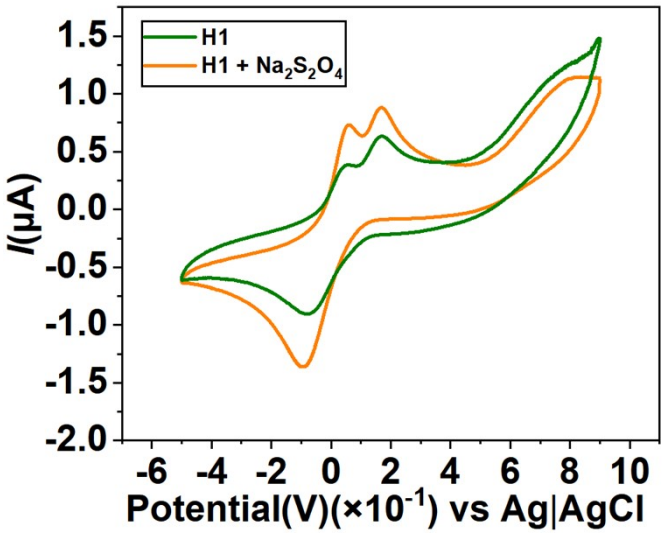

Fig. S2 Probe **H1** was used to identify the cyclic voltammetry curves before and after sodium dithionite in a 20 mM Tris-HCl buffer solution (pH=7.4) with the scan rate of 100 mVs^{-1} at 25±

0.5°C. Potentials are reported vs. Ag/AgCl (3 M KCl) reference electrode.

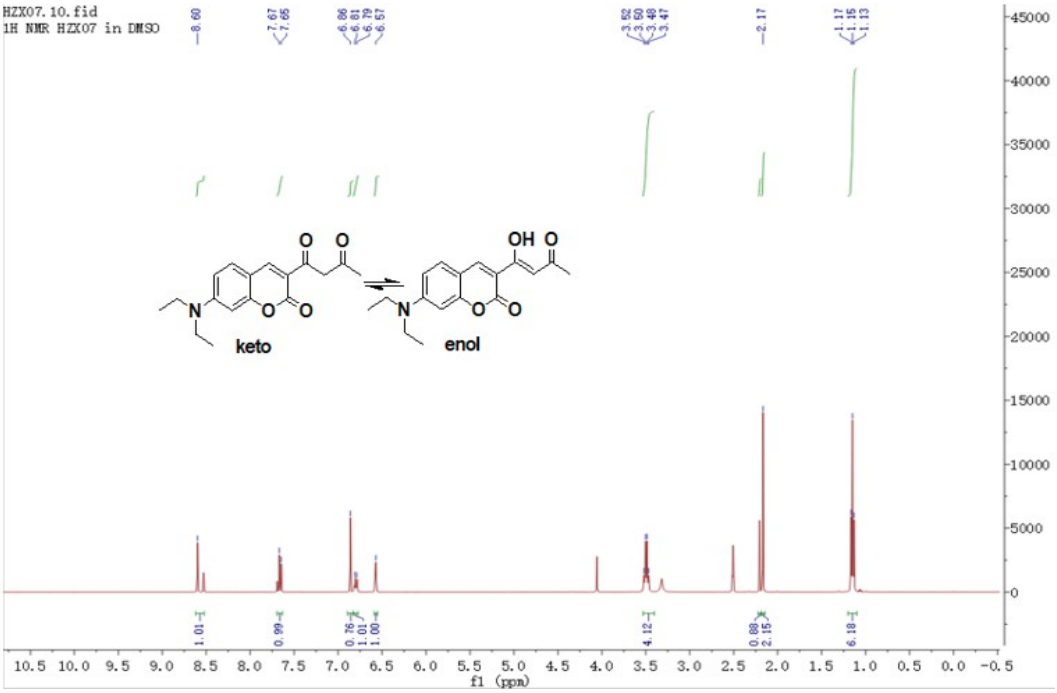

Fig. S3 ^{1}H NMR spectrum (DMSO-d_6, 400 MHz) of compound L1. Compound L1 is present in equilibrium between its enol (～85%) and keto (～15%) tautomers in DMSO-d_6

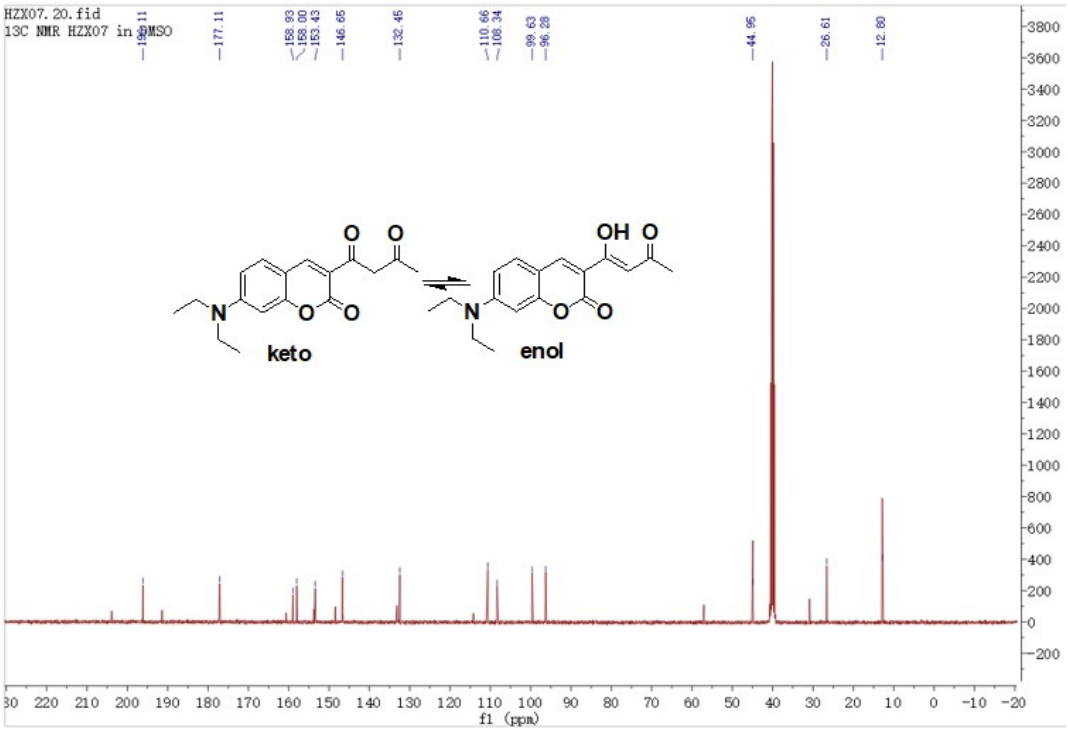

Fig. S4 ^{13}C NMR spectrum (DMSO-d_6, 101 MHz) of compound L1. Compound L1 is present in

equilibrium between its enol (～85%) and keto (～15%) tautomers in DMSO-d_6

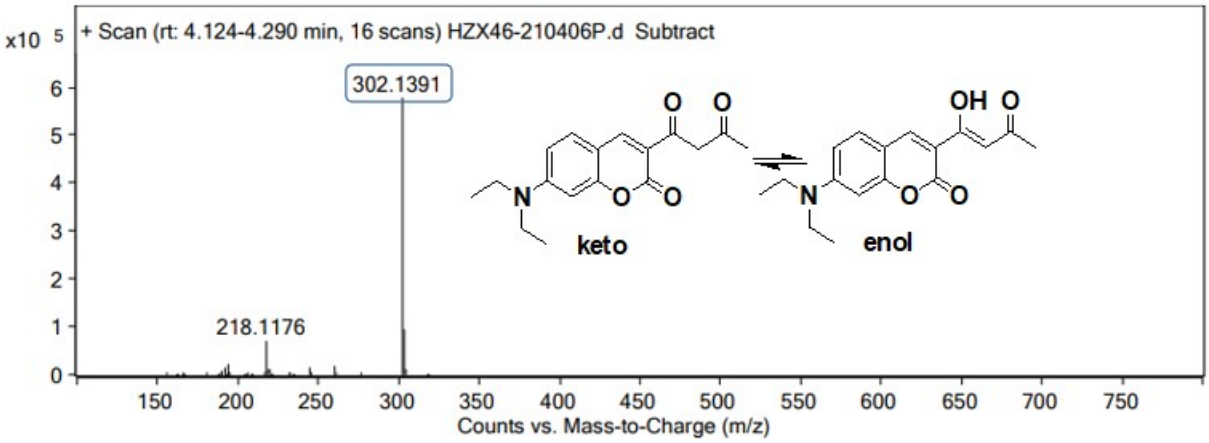

Fig. S5 Characterization of compound L1 by high resolution mass spectrometry, Compound L1 is present in equilibrium between its enol (～65%) and keto (～35%) tautomers in DCM

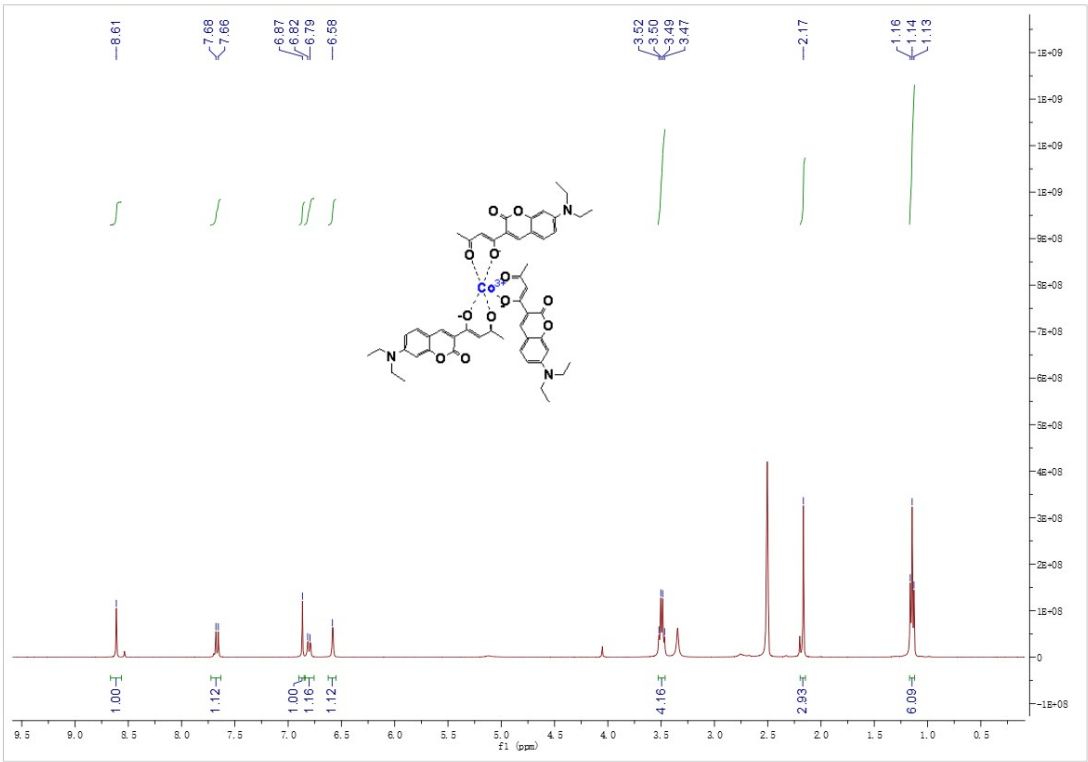

Fig. S6 ^{1}H NMR spectrum (DMSO-d_6, 400 MHz) of compound H1.

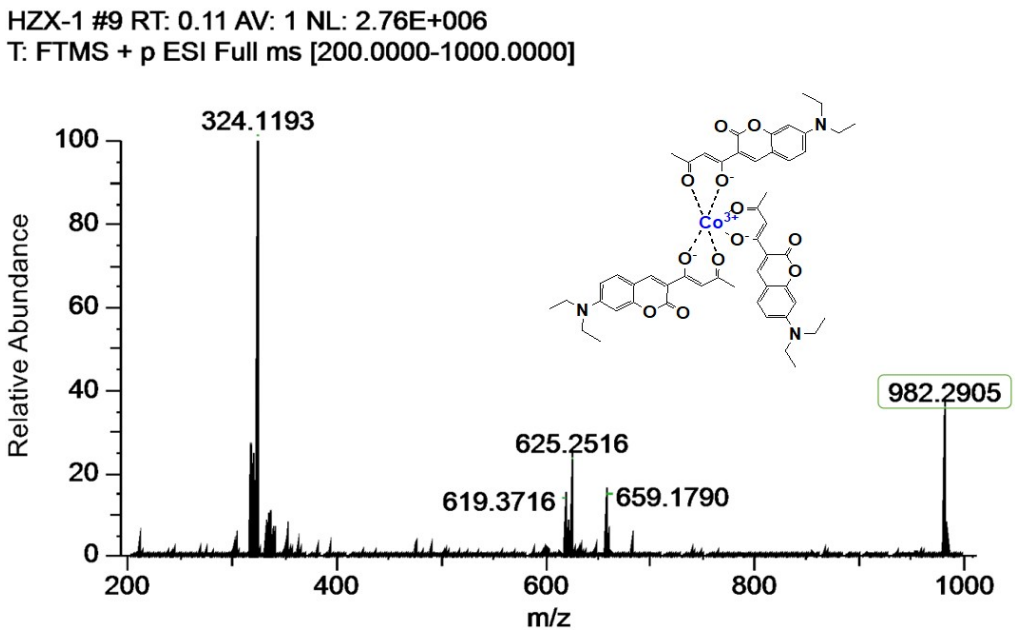

Fig. S7 Characterization of probe **H1** by high resolution mass spectrometry

Fig. S8 The color changes of **H1** (10 μM) in Tris aqueous buffer (DMF:Tris=1:9, 20 mM, pH=7.4) upon addition of various analytes (300 μM): 1. Blank,2. $S_2O_4^{2-}$, 3. HS^-, 4. Br^-, 5. Cl^-, 6. F^-, 7. HSO_3^-, 8. HSO_4^-, 9. S^{2-}, 10. NO_2^-, 11. NO_3^-, 12. $P_2O_7^{4-}$, 13. PO_4^{3-}, 14. SO_3^{2-}, 15. SO_4^{2-},16. H_2O_2, 17. Cys, 18. Hcy, 19.HClO, 20. $ONOO^-$)

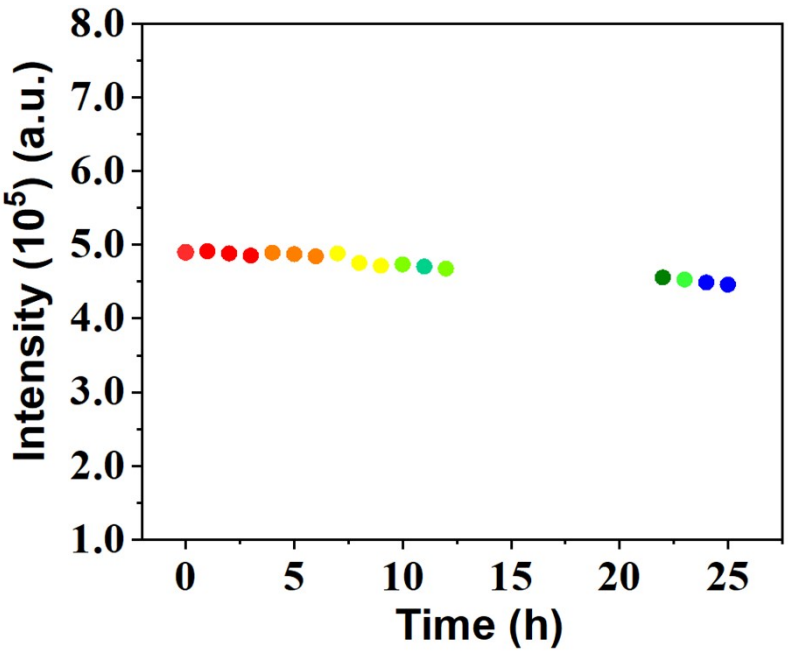

Fig. S9 The changes of fluorescence intensities of **H1** (10 μM) with time in Tris buffer solution (DMF:Tris=1:9, pH=7.4). λex=420 nm, λem=525 nm.

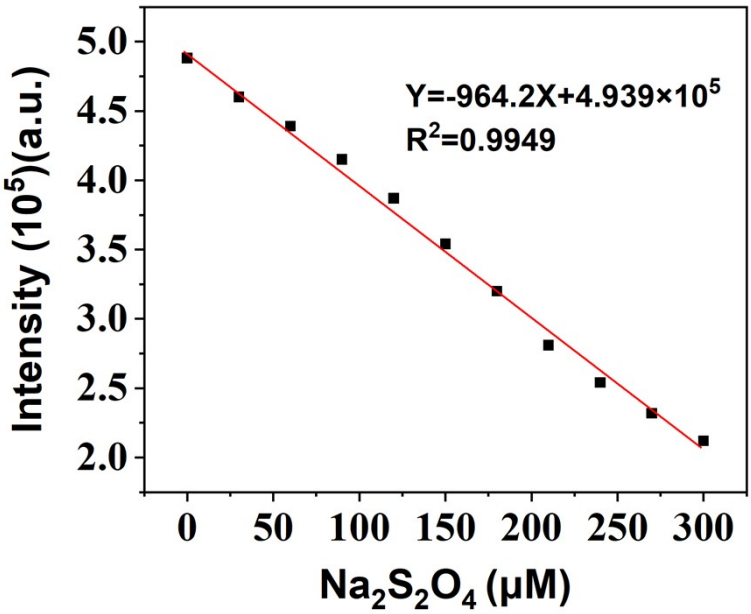

Fig. S10 Linear curve of emission intensity of **H1** (10 μM) at 525 nm versus $Na_2S_2O_4$ concentrations (0−300 μM).

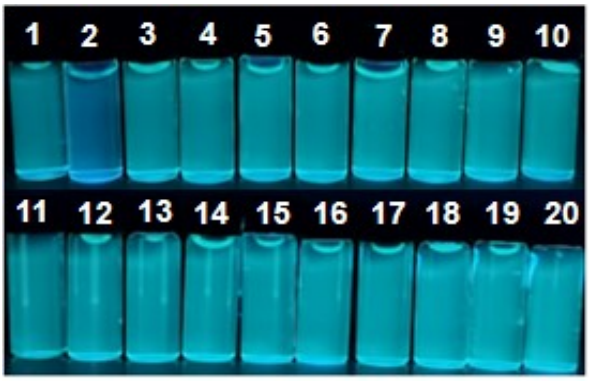

Fig. S11 Fluorescence colour photographs of **H1** (10 μM) in coexistence with analytes (300 μM) including 1. only **H1**, 2. $S_2O_4^{2-}$, 3. HS^-, 4. Br^-, 5. Cl^-, 6. F^-, 7. HSO_3^-, 8. S^{2-}, 9. NO_2^-, 10. NO_3^-, 11. $P_2O_7^{4-}$, 12. PO_4^{3-}, 13. SO_3^{2-}, 14. SO_4^{2-}, 15. GSH, 16. Hcy, 17. Cys, 18. $ONOO^-$, 19.HClO and 20. H_2O_2 under 365 nm UV lamp.

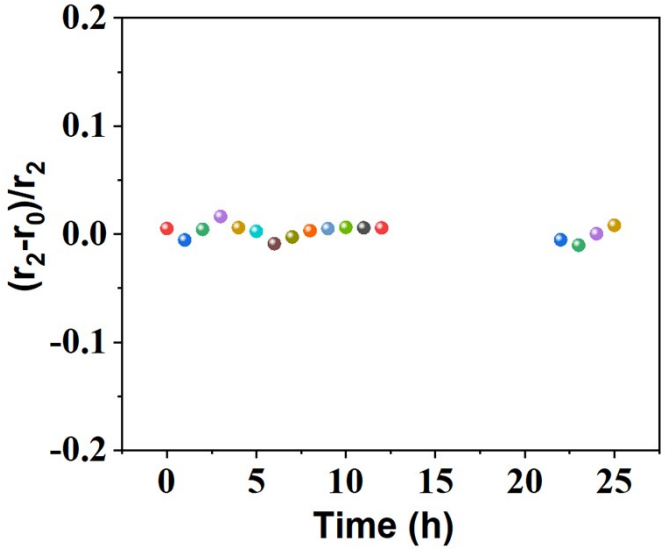

Fig. S12 Transverse relaxation rate (r_2) stability curve in the Tris-HCl buffer solution of the probe **H1** (10 μM)

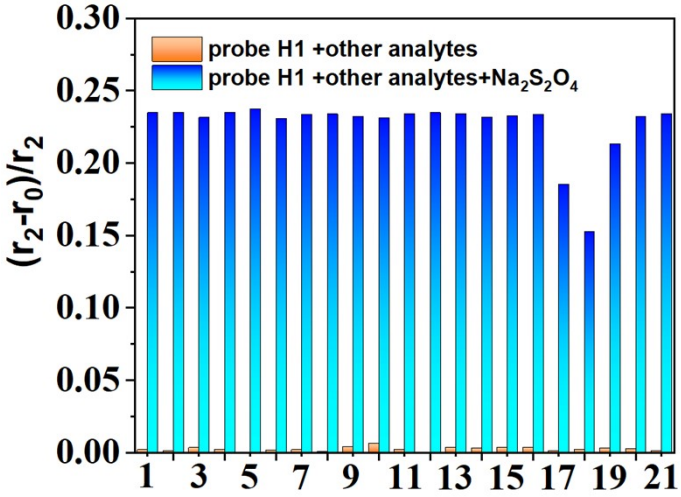

Fig. S13 Transverse relaxation rate (r_2) responses of **H1** (10 μM) towards $Na_2S_2O_4$ (300 μM) in

coexistence with analytes including 1. HS^-, 2. Br^-, 3. Cl^-, 4. F^-, 5. HSO_3^-, 6. S^{2-}, 7. NO_2^-, 8. NO_3^-, 9. $P_2O_7^{4-}$, 10. PO_4^{3-}, 11. SO_3^{2-}, 12. SO_4^{2-}, 13. GSH 14. Hcy, 15. Cys, 16. $ONOO^-$, 17.HClO and 18. H_2O_2 19.$S_2O_5^{2-}$, 20.$S_2O_3^{2-}$, and 21.CO_3^{2-}. (300 μM).

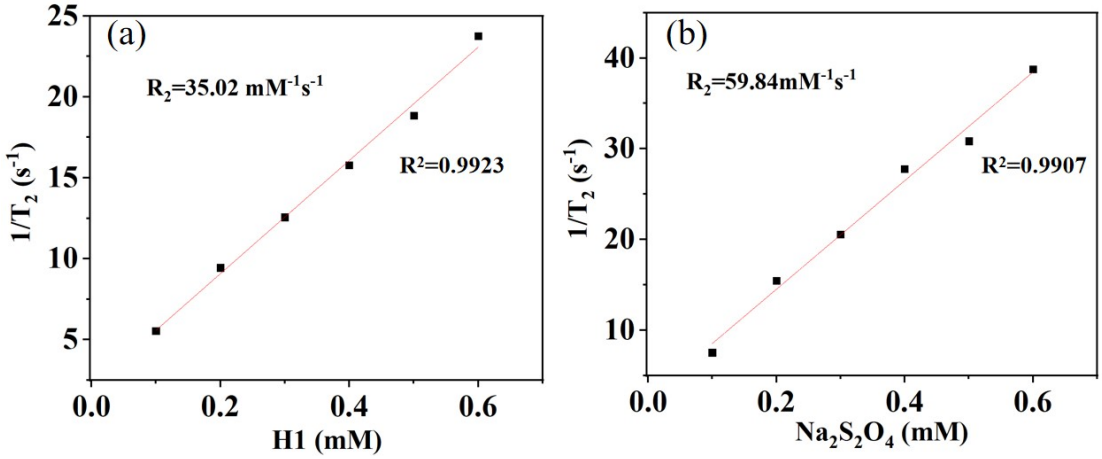

Fig. S14 Relaxation efficiency evaluation, (a) Co^{3+} complex under varying concentrations of **H1**. (b) Co^{2+} complex after reduction with $Na_2S_2O_4$.

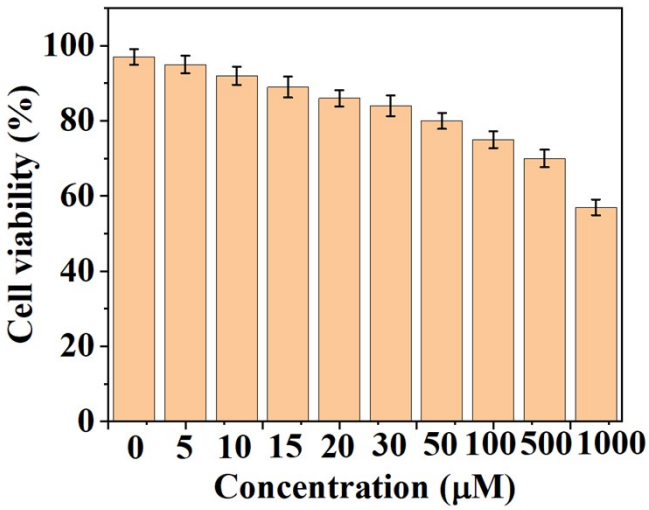

Fig. S15 Cytotoxicity of A549 cells after incubation with different concentrations of **H1** by MTT assay.

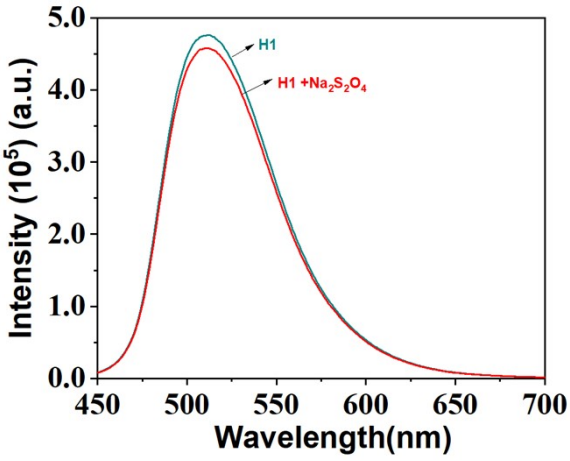

Fig. S16 Fluorescence emission spectra of **H1** (10 μM) in coexistence with $Na_2S_2O_4$ (300 μM, Exposed to air for 30 minutes) in Tris buffer with pH = 7.4, excitation: 420 nm.